Available online at www.sciencedirect.com
ScienceDirect
Procedia Engineering 2 (2010) 725–734
Procedia Engineering
www.elsevier.com/locate/procedia

Fatigue 2010

Multiaxial damage assessment and life estimation: application to an automotive exhaust manifold

Cristiana Delprete[a], Raffaella Sesana[a], Andrea Vercelli[a,*]

[a]*Politecnico di Torino, c.so Duca degli Abruzzi 24, Torino 10129, Italy*

Received 28 February 2010; revised 9 March 2010; accepted 15 March 2010

Abstract

Some mechanical components are subjected to thermo-mechanical fatigue, which occurs when both thermal and mechanical loads vary with time. Due to the complexity of the components geometry, stresses and strains field becomes multiaxial, worsening the fatigue resistance. In this paper several damage models are applied and compared on a case study, an automotive exhaust manifold simulacrum replying the material and the geometrical features of the commercial component. A complete thermo-structural FE analysis has been run and results have been post-processed by means of a numerical code implementing several multiaxial damage models available in literature and based both on a critical plane approach (Kandil-Brown-Miller, Fatemi-Socie) and strain-based models (Von Mises, ASME Code and Sonsino-Grubisic). The model calibration has been carried out by means of literature experimental data referred to commercial exhaust manifolds of similar geometry and material.

Keywords: Damage assessment; multiaxial; exhaust manifold; FEA; life estimation; thermo-mechanical fatigue.

1. Introduction

Life prediction is one of the most critical phases during the design procedure of a mechanical component. Stresses and strains computed by means of a complete structural analysis have to be post-processed in order to predict the component life. This procedure has to be performed before manufacturing component itself, allowing designers to make corrections during the design stage, when modifications are less costly.

A lot of approaches and models to treat the problem have been described in literature, taking into account as realistically as possible the phenomena and the influencing factors related to multiaxial fatigue, e.g. proportional or non proportional loadings, working temperature, materials characteristics including heat treatment, microstructure, anisotropy, environmental effects.

In this work different literature damage models suitable for treating low-cycle fatigue loading conditions have been applied and compared by post-processing stress and strain histories obtained from a complete non-linear transient FE analysis of a case study represented by an automotive exhaust manifold. By means of FAST-*Life*, a

* Corresponding author. *E-mail address*: andrea.verceli@polito.it

1877-7058 © 2010 Published by Elsevier Ltd.
doi:10.1016/j.proeng.2010.03.078

numerical code developed by the authors, the stress and strain histories in vectorial form are imported and processed according to the damage models chosen, giving the fatigue life as output.

All the required materials parameters have been extrapolated from literature and the resulting predictions have been compared to the experimental life of a similar actual component. The final aim of this research is indeed to propose a life estimation methodology, making a comparison between the damage models and giving a contribution to facilitate the model choice, a very tricky operation in the industrial field.

2. The FE model

In order to overtake any industrial confidentiality restrictions, a commercial cast iron exhaust manifold of a diesel IC engine has been purchased. In the machine shop of the Laboratory of Mechanical Engineering of the Politecnico di Torino this manifold has been dissected and geometrical features have been measured, building then the component model by means of Solidworks 2009 CAD software. To take into account the surrounding constraints of the manifold itself, the gasket, the bolts and a cylinder head simulacrum have been also modeled [1-5]. The procedure followed in this phase is represented in Figure 1.

(a) (b) (c)

Fig. 1. (a) The commercial exhaust manifold; (b) The cut sections; (c) The complete CAD model

The model has been then meshed with tetrahedral solid elements for the manifold, the gasket and the cylinder head simulacrum, while for bolts hexahedral elements have been used. The total number of nodes is 170828, whereas solid elements are 695175. Furthermore, in the thermal analysis, in which only temperature maps of the model are computed, first order elements have been adopted, switching the tetrahedral elements to the second order for the structural analysis to avoid the typical stiffness overestimation due to first order elements.

Contact interfaces have been also defined to simulate convective heat transfer between exhaust gas and the internal surfaces of the model, conductive heat transfer inside the components and between manifold and bolts, manifold and gasket, gasket and cylinder head and bolts and cylinder head. In the structural analysis also the friction contact between bolts, manifold, gasket and cylinder head has been taken into account.

To perform the thermo-structural FE analysis it has been hypothesized a SiMo cast iron for the manifold, two different types of steel for bolts and gasket, an aluminum alloy for high temperature applications for the cylinder head simulacrum. All the materials features adopted in the thermal analysis are summarized in the following Table 1, in which the references to literature works constitutive parameters have been extrapolated from are also reported.

Table 1. The thermo-physics properties of the materials considered in the thermal analysis

Manifold SiMo cast iron	Mass density [kg / m^3]	Conductivity [W / m K]	Specific heat [J / kg K]	References
20 °C	7100	48.5	460	[6,7]
200 °C	7100	48.5	460	[6,7]
400 °C	7100	48	510	[6,7]
600 °C	7100	47.7	536	[6,7]
800 °C	7100	47.7	536	[6,7]
Bolts steel AISI 4140	7900	97	480	[6,7]
Gasket steel AISI 301	8750	16.1	502	[6]
Cylinder head AlSi7 Aluminum alloy	2700	159	960	[6,7]

As shown in Table 1, for the cast iron temperature dependent parameters have been provided in order to predict the temperature map of the manifold; for the other materials temperature independent values of the parameters have been used because they are related to components which temperatures are not the first task.

In addition, Table 2 summarizes the materials parameters used in the structural analysis: as done for the thermo-physical properties, only the SiMo cast iron has been modeled with temperature dependent features. For what concerns the constitutive model, the cast iron behaviour is described by a non-linear isotropic hardening one, with a plastic slope represented by a straight line defined by the yield stress and the stress corresponding to a total strain equal to 5%, while the other materials are modeled as linear elastic due to the fact that their stresses are not of interest respect to the manifold ones.

Table 2. The structural properties of the materials characteristics considered in the structural analysis

Manifold SiMo cast iron	Young Modulus [GPa]	Poisson coefficient	Thermal expansion [1/ °C]	Yield stress [MPa]	Stress at 5% of strain [MPa]	References
20 °C	160	0.3	$12 \cdot 10^{-6}$	470	550	[1,6,7,8]
320 °C	145	0.3	$12 \cdot 10^{-6}$	405	510	[1,6,7,8]
480 °C	140	0.3	$12.7 \cdot 10^{-6}$	340	360	[1,6,7,8]
600 °C	125	0.3	$13.5 \cdot 10^{-6}$	180	185	[1,6,7,8]
930 °C	35	0.3	$14.2 \cdot 10^{-6}$	40	42	[1,6,7,8]
Bolts steel AISI 4140	200	0.3	$12.1 \cdot 10^{-6}$	-	-	[6,7]
Gasket steel AISI 301	193	0.3	$17 \cdot 10^{-6}$	-	-	[6]
AlSi7 Aluminum alloy	74.8	0.33	$21.5 \cdot 10^{-6}$	-	-	[6,7]

3. The FE thermo-structural analysis

The first step of the calculation is represented by a thermal transient analysis performed using the ABAQUS Version 6.8 commercial FE code to determine the temperature distribution on the component, hypothesizing that the environmental temperature is 70 °C, as actually measured in the engine compartment. In this phase convective heat exchange between exhaust gas and the internal surfaces of the model, and conductive heat exchange into the solids and through contacts are modeled.

As done in common practice [3, 9, 10], a typical trapezoidal thermal cycle replacing the exhaust gas temperature during a test-bench trials (maximum value of 740 °C and a period of 760 s) has been defined and repeated four times, so the total simulation time is 3040 s. To model also the cooling effects of the cylinder head, the cooling water temperature has been imposed through an amplitude curve defined as follows: a linear increase from 20 °C to 80 °C during the first 350 s of simulation, then a constant temperature of 80 °C until the end of the calculation.

Nodal temperature results have been stored into the database file every 50 s and in the following Figure 2 the thermal maps corresponding to the maximum temperature time instant are reported.

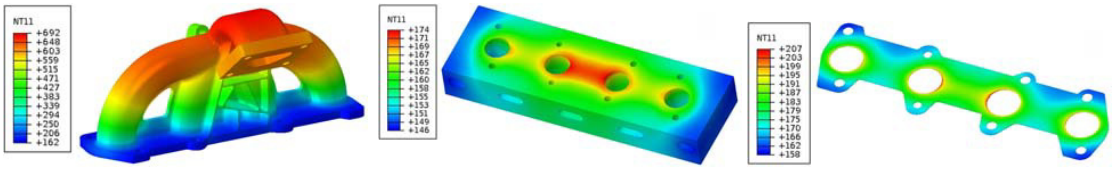

(a) (b) (c)

Fig. 2. The computed temperature distribution (in °C) of the exhaust manifold (a), the cylinder head simulacrum (b) and the gasket (c)

The nodal temperatures obtained by the thermal analysis have been then imported as initial conditions into the model for the transient structural analysis, in order to calculate stresses and strains generated by the application of

the thermal cycles. As explained in Section 2, the cast iron behaviour has been modeled using a non-linear isotropic hardening constitutive model, which parameters are temperature-dependent. The other materials have been modeled hypothesizing a linear elastic response because the analysis of the components related to is not the main goal of this work. The interactions between components have been taken into account specifying a friction contact condition.

As in the case of thermal analysis, also in this case the total simulation time is equal to 3040 s and the evolution of stresses and strains have been monitored for all the four thermal cycles imposed; the last cycle has been considered the stabilized one. Results have been stored every 50 s in terms of stresses, total and plastic strains and displacements; in the following Figure 3 an example of output from the structural analysis, corresponding to the maximum temperature time instant of the fourth thermal cycle imposed, is shown. For the same time instant the areas in which plastic strain occurs are depicted in Figure 4.

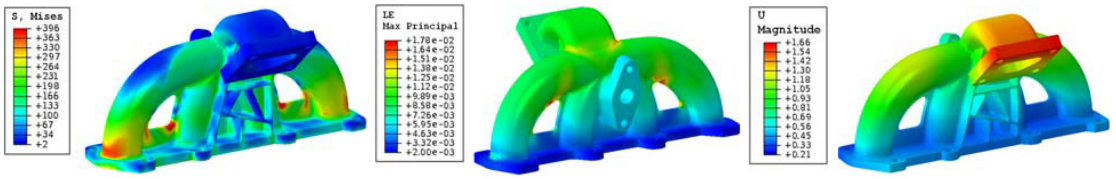

(a) (b) (c)

Fig. 3. The computed von Mises stress [MPa] (a), the total strain [mm/mm] (b) and the nodal displacements [mm] (c)

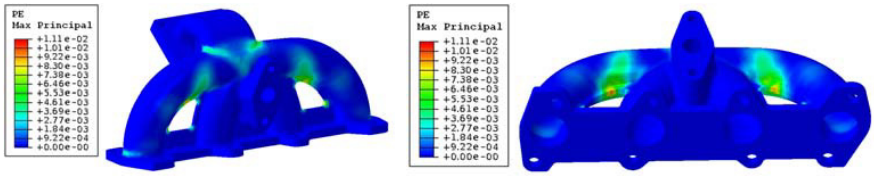

(a) (b)

Fig. 4. The areas in which plastic strain occurs [mm/mm] (a), and a detailed view of the widest ones (b)

The distribution of stresses and strains allows to identify the most critical areas for the structural integrity of the component during its working life. In this case these areas are set where the two external runners converge in the main collar, in the zone where the turbocharger collar is linked with the horizontal duct and, finally, in the areas between external and internal runners. Stresses and strains histories to be processed in order to estimate the fatigue life have been then extrapolated from these areas.

4. The damage models

In the following subsections the damage models used for life predictions are briefly illustrated. All the life estimation criteria suggest relations to calculate a value of uniaxial strain which can be considered equivalent to the multiaxial strain field. The correlation between this uniaxial equivalent strain and the number of cycles to failure is obtained through the Basquin-Manson-Coffin relation [11] represented by Eq. 1:

$$\varepsilon_{a,eq} = \frac{\sigma'_f}{E} \cdot \left(2N_f\right)^b + \varepsilon'_f \cdot \left(2N_f\right)^c \qquad (1)$$

Each multiaxial model provides therefore relations to calculate the term $\varepsilon_{a,eq}$ to use in Eq. 1 in which, when the fatigue strength coefficient σ'_f and exponent b and the fatigue ductility coefficient ε'_f and exponent c are known, the only unknown is the number of cycles to failure N_f. In order to use in a fast and easy way the damage models proposed, a dedicated numerical MATLAB®-based code have been developed by the authors [12, 13]: through

intuitive interactive windows the code, named FAST-*Life*, allows users to process stress and strain histories obtained by numerical simulations or experimental tests, elaborating them and giving the residual life according to each damage model adopted.

4.1. von Mises model

The von Mises model [14] is a strain based model, also known as the maximum octahedral shear strain amplitude criterion. For a multiaxial strain state, this hypothesis defines an equivalent strain amplitude $\varepsilon_{a,eq}$ according to Eq. 2:

$$\varepsilon_{a,eq} = \frac{1}{(1+\nu)\sqrt{2}} \cdot \left[\left(\varepsilon_{x,a} - \varepsilon_{y,a}\right)^2 + \left(\varepsilon_{x,a} - \varepsilon_{z,a}\right)^2 + \left(\varepsilon_{y,a} - \varepsilon_{z,a}\right)^2 + \frac{3}{2}\left(\gamma_{xy,a}{}^2 + \gamma_{xz,a}{}^2 + \gamma_{yz,a}{}^2\right) \right]^{\frac{1}{2}} \quad (2)$$

where $\varepsilon_{ij,a}$ and $\gamma_{ij,a}$ are respectively the normal and the shear strain amplitudes, while ν is the Poisson ratio.

4.2. ASME Code

The ASME Boiler and Pressure Vessel Code Procedure [15] prescribes to estimate life working on strain range instead of strain amplitude. Strain range is calculated as strain difference of two generic instants t_k and t_{k+1} of the strain history, e.g. $\Delta\varepsilon_{ij}(t) = \varepsilon_{ij}(t_k) - \varepsilon_{ij}(t_{k+1})$. The equivalent strain range is then calculated varying time instants in order to reach the maximum value of each strain range component; Eq. 3 shows the final relation.

$$\varepsilon_{a,eq} = \frac{1}{2} \cdot \max_t \left\{ \frac{\sqrt{2}}{3} \cdot \sqrt{\begin{array}{l} \left(\Delta\varepsilon_x(t) - \Delta\varepsilon_y(t)\right)^2 + \left(\Delta\varepsilon_x(t) - \Delta\varepsilon_z(t)\right)^2 + \left(\Delta\varepsilon_y(t) - \Delta\varepsilon_z(t)\right)^2 + \\ + 6 \cdot \left(\Delta\gamma_{xy}(t)^2 + \Delta\gamma_{xz}(t)^2 + \Delta\gamma_{yz}(t)^2 \right) \end{array}} \right\} \quad (3)$$

4.3. Sonsino-Grubisic model

The criterion of Sonsino and Grubisic [16] assumes that fatigue damage is caused by the interaction of shear strains acting on different elementary material planes, called interference planes, univocally defined by the spherical coordinates θ and φ, by the unit normal vector **n**, and the free material surface *dA*, as shown in Figure 5.

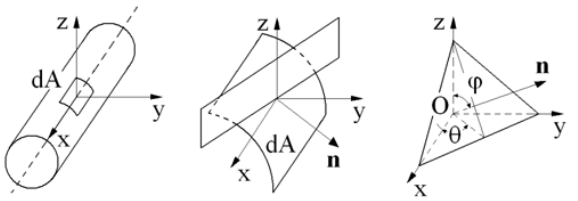

Fig. 5. Definition of the interference plane

The calculation of the shear strain value which acts on each interference plane is simplified, according to Sonsino and Grubisic, considering only the coordinate θ and the time instant t, working on planes normal to the surface so that φ assumes a constant value of 90°. For each time instant the shear strain is then determined by Eq. 4:

$$\gamma(\theta, t) = \left(\varepsilon_x(t) - \varepsilon_y(t)\right) \cdot sin(2\theta) + \gamma_{xy}(t) \cdot cos(2\theta) \quad (4)$$

The shear amplitude is then calculated for each plane maximizing the difference between shear strains corresponding to the different time instants under consideration, as shown by Eq. 5.

$$\gamma_a(\theta_i) = \frac{1}{2} \cdot \left[\max_t\left(\gamma(\theta_i, t)\right) - \min_t\left(\gamma(\theta_i, t)\right) \right] \quad (5)$$

Next the arithmetic mean value of the shear strain amplitudes determined by Eq. 5 has to be calculated:

$$\gamma_{a,arith} = \frac{1}{\pi} \cdot \int_0^{\pi} \gamma_a(\theta) d\theta \tag{6}$$

Finally, Eq. 7 gives the equivalent axial strain amplitude to use into the Basquin-Manson-Coffin relation:

$$\varepsilon_{a,eq} = \frac{5}{4 \cdot (1+\nu)} \cdot \gamma_{a,arith} \tag{7}$$

4.4. Kandil-Brown-Miller model

The Kandil-Brown-Miller criterion has been developed adopting a critical plane approach, justified by experimental observations of the nucleation and growth of cracks during loading: depending on the material, stress state, environment, and strain amplitude, fatigue life is usually dominated by crack growth along either shear planes or tensile planes [14]. Kandil, Brown and Miller proposed that both the cyclic shear and normal strain on the plane of maximum shear must be considered due to the fact that cyclic shear strains help to nucleate cracks, while normal strains contribute in their growth [17].

Referring to the Mohr circles, the maximum shear strain amplitude $\Delta\gamma_{max}$ and the normal strain rate $\Delta\varepsilon_n$ are:

$$\frac{\Delta\gamma_{max}}{2} = \frac{\varepsilon_1 - \varepsilon_3}{2} \qquad \text{and} \qquad \Delta\varepsilon_n = \frac{\varepsilon_1 + \varepsilon_3}{2} \tag{8}$$

where ε_1 and ε_3 are respectively the maximum and the minimum principal strain. Since $\varepsilon_3 = -\nu\varepsilon_1$, the maximum shear strain amplitude and the normal strain rate can be also written as in Eq. 9:

$$\frac{\Delta\gamma_{max}}{2} = \frac{\varepsilon_1 - \varepsilon_3}{2} = \frac{\varepsilon_1 \cdot (1+\nu)}{2} \qquad \text{and} \qquad \Delta\varepsilon_n = \frac{\varepsilon_1 + \varepsilon_3}{2} = \frac{\varepsilon_1 \cdot (1-\nu)}{2} \tag{9}$$

The equivalent shear strain amplitude used to replace the axial strain amplitude into the Basquin-Manson-Coffin relation is then represented by Eq. 10.

$$\gamma_{a,eq} = \frac{\Delta\gamma_{max}}{2} + \frac{\Delta\varepsilon_n}{2} \tag{10}$$

The Basquin-Manson-Coffin which has to be use according to the Kandil-Brown-Miller criterion is modified respect to the original formulation of Eq. 1 by the addition of two other coefficients C_1 and C_2, as shown in Eq. 11.

$$\varepsilon_{a,eq} = C_1 \frac{\sigma_f'}{E} \cdot (2N_f)^b + C_2 \varepsilon_f' \cdot (2N_f)^c \tag{11}$$

For most of the common metallic materials in the elastic field, the Poisson coefficient can be considered equal to 0.3, so the strain components under investigation assume the form of Eq. 12.

$$\Delta\gamma_{max} = \varepsilon_1 \cdot (1+\nu) = 1.3 \cdot \varepsilon_1 \qquad \text{and} \qquad \Delta\varepsilon_n = \varepsilon_1 \cdot (1-\nu) = 0.35 \cdot \varepsilon_1 \tag{12}$$

From these considerations it follows that $C_1 = 1.3 + 0.35 = 1.65$ and, through the same methodology adopted for the elastic field, the parameter associated to the plastic field ($\nu = 0.5$) becomes $C_2 = 1.75$. The final equation to be used in for life estimation according to Kandil-Brown-Miller is then presented in Eq. 13.

$$\frac{\Delta\gamma_{max}}{2}+\frac{\Delta\varepsilon_n}{2}=1.65\cdot\frac{\sigma'_f}{E}\cdot\left(2N_f\right)^b+1.75\cdot\varepsilon'_f\cdot\left(2N_f\right)^c \tag{13}$$

4.5. Fatemi-Socie model

This model was born as a modification of the Brown-Miller's critical plane model, considering mainly the maximum shear strain amplitude and the maximum normal stress on the maximum shear strain amplitude plane [18]. Considering the normal stress also the crack closure effects which may derived from the application of cyclic loadings can be taken into account. The fatigue parameter to be used in life prediction is then defined by Eq. 14:

$$\gamma_{a,eq}=\frac{\Delta\gamma_{max}}{2}\left(1+n\frac{\sigma_{n,max}}{\sigma_y}\right) \tag{14}$$

where $\sigma_{n,max}$ is the maximum normal strain on the maximum shear strain amplitude plane, σ_y is the yield stress, n is a material constant which can be found by fitting the uniaxial experimental data against the pure torsion data. In order to use this fatigue parameters, the shear strain formulation of the Basquin-Manson-Coffin equation (Eq. 15) has to be used, in which it can be applied the axial and shear properties $\tau'_f \approx \sigma'_f / 3^{1/2}$, $b_\gamma \approx b$, $\gamma'_f \approx \varepsilon'_f / 3^{1/2}$ and $c_\gamma \approx c$ [19].

$$\frac{\Delta\gamma_{max}}{2}\left(1+n\frac{\sigma_{n,max}}{\sigma_y}\right)=\frac{\tau'_f}{G}\cdot\left(2N_f\right)^{b_\gamma}+\gamma'_f\cdot\left(2N_f\right)^{c_\gamma} \tag{15}$$

5. The life estimations

As stated in Section 3, in order to estimate the residual life of the manifold stress and strain histories corresponding to the most critical zones have been extracted from the results database; these data are referred to the fourth simulated thermal cycle, which can be considered a good representation of the stabilized conditions. For each critical area shown in Figure 6 a single element has been investigated.

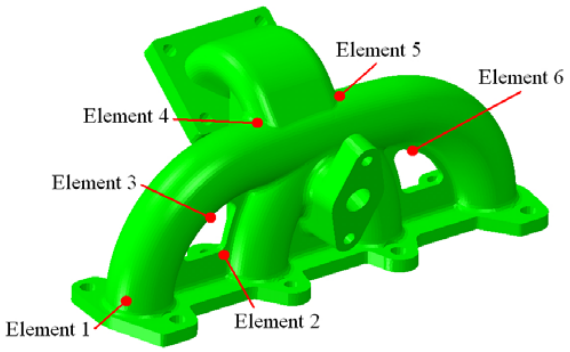

Fig. 6. Areas under investigation for life prediction

From the results database the six components of stress and strain tensors have been then extracted and formatted as text files to be imported into the damage assessment numerical code FAST-*Life* [13]. These data have been processed using all the damage criteria illustrated in Section 4 and the estimated lives in terms of number of cycles to failure have been compared.

In order to verify the reliability of the computed predictions, life estimations have been also compared with the mean experimental life available in literature for a very similar commercial exhaust manifold, characterized by the same geometrical features of the present simulacrum (in terms of number of runners, general dimensions,

thicknesses, presence of EGR and turbocharger collars) and subjected to similar thermal cycles of the present study. The following Table 3 summarizes the obtained results.

Table 3. The number of cycles to failure predicted by the proposed damage models

Element	von Mises	ASME code	Sonsino-Grubisic	Kandil-Brown-Miller	Fatemi-Socie	Experimental life [1, 20]
1	7690	7820	8790	7410	9180	3400
2	8230	8380	9920	7970	> 10000	
3	4100	4210	**4820**	**3780**	**5030**	
4	> 10000	> 10000	> 10000	> 10000	> 10000	
5	**3960**	**4080**	5210	3920	5610	
6	4140	4300	4930	3860	5120	

As reported in Table 3, the string >10000 means that the stress-strain field is not damaging enough to cause failure in LCF regime, commonly assumed to be corresponding to the range 0-10^4 cycles.

Focusing the attention on the most critical elements identified by the damage model used, it is possible to see that their predicted lives are comparable to the experimental one. Moreover, the most critical element of the component, that is the element to which the shortest life is associated, may in general vary according to the different models, due to the fact that the stress-strain fields are processed in different ways respect to the analytical approach adopted by each model, such that from the same stress-strain data can result different damages.

The comparison between the number of cycles to failure predicted and the experimental life highlights that the most reliable estimation can be obtained by the Kandil-Brown-Miller model, which is also the most conservative one, and by the von Mises model, which differ each other in that the estimated critical element is not the same. The ASME code gives an higher fatigue life, while the Sonsino-Grubisic and the Fatemi-Socie models provide the most optimistic life predictions.

In general, the damage models analyzed in this study are all applicable in low-cycle fatigue and in thermo-mechanical fatigue regime, both with in-phase and out-of-phase loading paths [14, 21]; however, some remarks have to be done for each model. The major drawback resulting from the hypothesis of von Mises is that it produces the same equivalent strain for both the in-phase and out-of-phase loading conditions and, consequently, both load states cause the same fatigue life according to von Mises model. Experimental observations contradict this prediction, demonstrating that out-of-phase loading paths are in general most damaging than in-phase ones; von Mises criterion may then result non conservative for out-of-phase thermo-mechanical loading cases.

The ASME code is developed starting from the same constitutive hypotheses of the von Mises criterion, but it produces a lower equivalent strain for the out-of-phase than for the in-phase loading [21], in contradiction with experimental results. This fact can lead to non conservative predictions, as come out also from this study in which ASME code predictions are more optimistic than the von Mises ones.

The Sonsino-Grubisic criterion is based on the analysis of the shear strain acting on the interference planes, taking into account neither the interactions between normal and shear strain path nor stress gradient [21]. This is the reason why this model can results non-conservative if the stress gradient effect is beneficial for fatigue life, or optimistic if stress gradient is damaging.

The Fatemi-Socie criterion is focused on the shear strain and takes into account also the contribution of the normal stress in order to avoid the major disadvantage of the critical plane models that include only shear terms, which can not reflect the effect of mean stress or strain path dependent hardening. Fatemi-Socie model can explain the difference between damage effects in tension and torsion loading and can be used to describe mean stress and non-proportional hardening effects. However it has been demonstrated that for ductile metallic materials the best correlation with experimental data can be achieved using a critical plane model which takes into account the normal strain instead of the normal stress [14].

The multiaxial damage model proposed by Kandil-Brown-Miller computes the equivalent strain processing both shear and normal strains. This hypothesis is coherent with reality because on the critical plane both normal and shear

strain occur for ductile materials. In addition, this model can also take into account mean stress effects and it results to be the most suitable one for fatigue applications when large strain occurs in ductile metals.

6. Conclusion

The present study is focused on the comparison between the estimated lives obtained through the von Mises, the ASME code, the Sonsino-Grubisic, the Kandil-Brown-Miller, and the Fatemi-Socie multiaxial damage assessment criteria. These predictions have been also compared with the experimental life available in literature of an actual commercial exhaust manifold, very similar to the simulacrum analyzed in this work in terms of geometrical features and loading conditions.

A numerical code developed by the authors, named FAST-*Life* and implementing the analytical expressions constituting the proposed criteria, has been used to perform life predictions. The aim of the code is to process the stress-strain data computed by simulations according to the different damage models used, giving as output the number of cycles corresponding to each area analyzed, after the required constitutive material parameters have been specified.

In the present study, stress and strain fields have been computed through a complete FE thermo-structural transient analysis of an automotive exhaust manifold simulacrum. All the constitutive material parameters required by the analyses performed have been found in literature.

The results achieved by the life prediction activity allow to draw the following conclusions:

1. life predictions are obviously different in terms of number of cycles to failure depending on the damage model used, but also the most damaged zone may vary due to the fact that the same stress-strain field causes different damage depending on the approach adopted by the model used for life estimation;
2. the damage model which gives the most conservative life predictions is the Kandil-Brown-Miller one, which takes into account both shear and normal strain acting on the critical plane and, for this reason, it results to be particularly suitable for ductile metallic materials in LCF thermo-mechanical regime;
3. life estimations are comparable to the experimental life of the actual component, confirming that the damage assessment procedure followed in this study can be considered a valid methodology to predict life for high temperature and high strain fatigue applications;
4. even if the damage models here adopted are all applicable to predict residual life of components subjected to high temperature and high strain fatigue, the analysis of both the results obtained and the specific literature allows to state that the Kandil-Brown-Miller can be considered the most suitable damage model between those proposed in this study;
5. one of the major advantage of all the damage models investigated in this study is that only four constitutive material parameters have to be estimated in order to calibrate the Basquin-Manson-Coffin relation, allowing to save money and time for experimental tests campaigns.

In conclusion, in the present study a methodology to predict residual life under multiaxial stress-strain field has been proposed, comparing life estimations obtained by several damage models applied to the stress-strain data computed by FE simulations. In order to overtake any industrial confidentiality restrictions, an appropriate case study represented by an exhaust manifold simulacrum has been used, extrapolating all the required material properties and loading conditions from literature. The results obtained have allowed to identify the most suitable damage model between the most known ones, and they justify the adoption of this methodology for high temperature LCF loading conditions.

The next step of this research activity will be the fulfillment of a complete experimental test campaign in order to rigorously calibrate all the constitutive material parameters, achieving a higher quality of the thermo-structural simulations results and, consequently, of the life estimations.

References

[1] Costantinescu A, Charkaluk E, Lederer G, Verger L. A computational approach to thermomechanical fatigue. *International Journal of Fatigue* 2004;**26**:805-818

[2] Hazime RM, Dropps SH, Anderson DH, Ali MY. Transient non-linear FEA and TMF life estimation of cast exhaust manifolds. *SAE Technical Paper* 2003; 2003-01-0918

[3] Wohrmann R, Seifert T, Willeke W, Hartmann D. Fatigue life simulation for optimized exhaust manifold geometry. *SAE Technical Paper* 2006; 2006-01-1249

[4] Mamiya N, Masuda T, Noda Y. Thermal fatigue life of exhaust manifold predicted by simulation. *SAE Technical Paper* 2002; 2002-01-0854

[5] Baldissera P, Delprete C, Rosso C. Numerical and experimental analysis of exhaust manifold gasket. *SAE Technical Paper* 2006; 2006-01-1210

[6] Brandes EA, Brook GB. *Smithells Metal Reference Book*. Oxford: Butterworth-Heinemann; 1992

[7] Druschitz AP, Fitzerald DC. Lightweight iron and steel castings for automotive applications. *SAE Technical Paper* 2000; 2000-01-0679

[8] Anderson DH, Bisaro DR, Haan DM, Olree M. A thermoviscoplastic FE model for the strain prediction in high temperature, thermal cycling applications for silicon molybdenum nodular cast iron. *SAE Technical Paper* 1998; 980697

[9] Delprete C, Rosso C. Exhaust manifold thermo-structural simulation methodology. *SAE Technical Paper* 2005; 2005-01-1076

[10] Su X, Zubeck M, Lasecki J, Engler-Pinto Jr CC, Tang C, Sehitoglu H, Allison J. Thermal fatigue analysis of cast aluminum cylinder heads. *SAE Technical Paper* 2002; 2002-01-0657

[11] S. S. Manson. *Thermal Stress and Low Cycle Fatigue*. New York: Mc Graw-Hill; 1966

[12] Delprete C, Rosso C, Sesana R, Vercelli A. Sviluppo di un codice di calcolo per la stima della durata a fatica termomeccanica. *XXXVII Convegno AIAS*, Roma, Italy, 2008 (in italian)

[13] Delprete C, Rosso C, Sesana R, Vercelli A. Sviluppo di un codice di calcolo per la stima della durata a fatica multiassiale. *XXXVIII Convegno AIAS*, Torino, Italy, 2009 (in italian)

[14] D. F. Socie, G. B. Marquis. *Multiaxial Fatigue*. Warrendale: SAE International; 2000

[15] ASME. Class 1: components in elevated temperature service. *Cases of ASME Boiler and Pressure Vessel Code*. Section III, Division 1, Appendix T. New York; 2007

[16] Sonsino CM, Grubisic V. Fatigue behaviour of cyclically softening and hardening steels under multiaxial elastc-plastic deformation. In: Brown MW, Miller KJ, editors. *Multiaxial fatigue, ASTM STP 853*, Philadelphia: Eds. American Society for Testing and Material; 1985, p. 586-605

[17] Kandil FA, Brown MW, Miller KJ. Biaxial low-cycle fatigue fracture of a 316 stainless steel at elevated temperature. *The Metals Society, Book 280*. London; 1982

[18] Fatemi A, Socie DF. A critical plane approach to multiaxial fatigue damage including out-of-phase loading. *Fatigue Fract. Engng Mater. Struct*. 1988;**11** (3):149-165.

[19] Socie DF. Critical planes approaches for multiaxial fatigue damage assessment. In: McDowell DL, Ellis R, editors. *Advances in multiaxial fatigue*, *ASTM STP 1191*, Philadelphia: Eds. American Society for Testing and Material; 1993, p. 7–36

[20] Lederer G, Charkaluk E, Verger L, Constantinescu A. Numerical lifetime assessment of engine parts submitted to thermomechanical fatigue, application to exhaust manifold design. SAE Technical Paper 2000; 2000-01-0789

[21] Filippini M, Foletti S, Papadopoulos IV, Sonsino CM. A multiaxial fatigue life criterion for non-symmetrical and non-proportional elasto-plastic deformation. In: Carpinteri A, de Freitas M, Spagnoli A, editors. *Biaxial/Multiaxial Fatigue and Fracture*, Eds. Elsevier ESIS Publication 31; 2003, p. 383-400